JACS ARTICLES

Published on Web 07/20/2010

Self-Assembly and Induced Circular Dichroism in Dendritic Supramolecules with Cholesteric Pendant Groups

Antti J. Soininen,[†] Edis Kasëmi,[‡] A. Dieter Schlüter,[‡] Olli Ikkala,[†] Janne Ruokolainen,*[,†] and Raffaele Mezzenga*[,§]

Department of Applied Physics, Aalto University School of Science and Technology, 02150 Espoo, Finland, Department of Materials, Laboratory of Polymer Chemistry, ETH Zurich, 8093 Zürich, Switzerland, and Institute of Food Science & Nutrition, ETH Zurich, 8092 Zürich, Switzerland

Received May 3, 2010; E-mail: Janne.Ruokolainen@tkk.fi; Raffaele.Mezzenga@agrl.ethz.ch

Abstract: We report on the solid-state structural features of self-assembled chiral supramolecules based on ionic complexation of chiral cholesteric pendant groups with achiral dendritic macromolecules and show that their optical activity exhibits a systematic change in the ultraviolet/visible light (UV−vis) absorption and enhancement in the circular dichroism (CD) signal, indicating the occurrence of supramolecular chirality, also referred to as induced circular dichroism (ICD). We construct a homologous series of complexes by varying systematically from 1 to 3 the generation of dendritic units contained in dendrons, dendrimers, and dendronized polymers. The structural properties of the complexes are investigated by means of small-angle X-ray scattering (SAXS) and transmission electron microscopy (TEM). Depending on the class of dendritic molecule and the generation, lamellar, columnar hexagonal, oblique columnar, and rectangular columnar phases can be found, with a direct correlation among the degrees of freedom of the dendritic macromolecules used and the level of order achieved in the self-assembled solid-state structures. The enhancement of the optical signals of these mesoscopic structures appears to be correlated with their order in the solid state. Complexes with the longest lattice correlation lengths also show the most enhanced CD signals. These results show the unique versatility of dendritic macromolecules as supramolecular templates capable of organizing low molecular weight chiral pendant units into a variety of solid-state structures with amplified optical properties.

Introduction

Noncovalent binding of side chains to polymer backbones is a powerful tool for designing polymer systems with complex topologies at the mesoscopic length scale.[1−3] By exploitation of the dynamic and reversible nature of physical bonds and the different energies that hold together side chains and polymers, as well as the multitudes of molecular architectures available for both the macromolecular templates and side chains, new materials with unprecedented properties can be created.[4] The self-assembly behavior resulting from microphase separation occurring among noncovalently bound side chains and polymer backbones is an interplay between the immiscibility of pendant groups and the polymer backbone, the minimization of energy associated with creation of new interfaces, and the reduction of conformational entropy associated with restricted configurations of macromolecular backbones. If the side chains are mesogenic, an additional conformational driving force arises from the presence of liquid crystalline interactions. As a result of this complex behavior, these materials show properties inherent to both their polymeric nature and the liquid crystalline side groups.

Dendrons and dendrimers have a perfectly defined macromolecular architecture, in the sense that they possess 100% degree of branching, a fractal-like structure, and monodisperse molecular weights. As a consequence, they typically bear a large and defined number of functionalized groups in their outer shell. Their molecular conformations and properties are different from those of other macromolecules, since with increasing generation, they become larger and bulkier and contain an increasing number of peripheral units.[5−9] On the other hand, dendronized polymers, that is, linear polymers with dendritic side chains attached to each individual repeat unit of a polymer backbone, combine features of both dendritic molecules and linear polymers.[10−13] The polymer backbone may impose additional restrictions on the self-assembly process of the pendant dendritic side chains as compared to nonbonded dendrons and dendrim-

[†] Aalto University School of Science and Technology.
[‡] Department of Materials, Laboratory of Polymer Chemistry, ETH Zurich.
[§] Institute of Food Science & Nutrition, ETH Zurich.

(1) ten Brinke, G.; Ruokolainen, J.; Ikkala, O. *Adv. Polym. Sci.* **2007**, *207*, 113–177.
(2) Pollino, J. M.; Weck, M. *Chem. Soc. Rev.* **2005**, *34*, 193–207.
(3) Weck, M. *Polym. Int.* **2007**, *56*, 453–460.
(4) Hammond, M. R.; Mezzenga, R. *Soft Matter* **2008**, *4*, 952–961.
(5) Al-Jamal, K. T.; Ramaswamy, C.; Florence, A. T. *Adv. Drug Delivery Rev.* **2005**, *57*, 2238–2270.
(6) Smith, D. K.; Hirst, A. R.; Love, C. S.; Hardy, J. G.; Brignell, S. V.; Huang, B. Q. *Prog. Polym. Sci.* **2005**, *30*, 220–293.
(7) Vögtle, F.; Gestermann, S.; Hesse, R.; Schwierz, H.; Windisch, B. *Prog. Polym. Sci.* **2000**, *25*, 987–1041.
(8) Tomalia, D. A. *Prog. Polym. Sci.* **2005**, *30*, 294–324.
(9) Barbera, J.; Donnio, B.; Gehringer, L.; Guillon, D.; Marcos, M.; Omenat, A.; Serrano, J. L. *J. Mater. Chem.* **2005**, *15*, 4093–4105.
(10) Zhang, A.; Shu, L.; Bo, Z.; Schlüter, A. D. *Macromol. Chem. Phys.* **2003**, *204*, 328–339.

 10.1021/ja103754d

ers.[13] A thorough review of the self-organization and self-assembly of dendritic systems is available.[14]

Liquid cystalline self-assembled materials have great potential in applications where dynamic and functional materials are required.[15] Recently, we have shown that dendrons, dendrimers, and dendronized polymers can be used as efficient macromolecular templates to yield, via supramolecular self-assembly, nanostructured liquid crystalline polymers with unconventional solid-state structures. In these systems, the structure and period can be fine-tuned either by the dendron generation or by the size of the surfactants bound noncovalently to the dendron periphery.[16−19] Most importantly, it was discovered that the columnar structures encountered in these supramolecular systems are "inverted" in the sense that the dendritic molecules occupy the continuous domains while the surfactants are confined in discrete domains: although these findings may appear counterintuitive given the natural curvature of the dendritic molecules, the inverted configuration has been univocally demonstrated both experimentally and theoretically.[18−21]

In side-chain polymers, chiral pendant groups attached to a racemic or achiral polymer backbone may induce a chiral conformation in the polymer. This "chirality driving force" can be utilized in supramolecular host−guest systems where chiral guest molecules induce chirality in an achiral host or vice versa.[22] Work for "memorizing", that is, freezing the chiral conformation of host molecules when the chiral guest molecules are removed from the complex, was pioneered by Yashima et al.[23] in polymer solutions. Since then the memory effect has been shown to function in many supramolecular systems. Relatively small molecules,[24] polymers[25−33] and supramolecular assemblies[34] among others can act as a host. The phenomenon is not only limited to solutions; for example, chirality memorizing thin films[35] and gels[36] have been studied. In addition to chirality sensing and optically active materials, the memory effect can be utilized in, for example, stereoselective catalysis.[37]

In self-assembling dendritic systems, the introduction of chiral elements to dendritic molecules results in chiral molecular assemblies. Work by Percec and co-workers[13,38−43] has been very fruitful in this field; his group has analyzed chiral dendritic systems that have columnar or, in some cases, spherical morphology depending on the "effective" shape of the dendritic moieties. It is interesting to note that the columnar assemblies often exhibit a central pore in the above-mentioned work. The induction of chirality in noncovalently bound dendritic systems has also received attention: for example, Tsiourvas et al.[44] have complexed cholesteric moieties with amine-terminated poly(propylenimine) dendrimers and the complexes exhibited a chiral smectic C phase. In this study, we address for the first time the effect of dendritic molecular architecture on the solid-state morphology and induced circular dichroism (ICD) of supramolecular dendritic ionic systems. The chiral behavior is triggered by sulfate cholesteric groups ionically attached to the periphery of cationic dendritic macromolecules. In order to systematically change the architecture of the macromolecular template, we use dendrons, dendrimers, and dendronized polymers of generations varying from one to three. The templates are based on the exact same branching unit so as to achieve maximum comparability. This leads to a homologous library of dendritic supramolecule−cholesteric complexes constituted by nine different cases. The results are interpreted in terms of small-angle X-ray scattering (SAXS), transmission electron microscopy (TEM), ultraviolet/visible light spectroscopy (UV−vis), and circular dichroism (CD).

Results and Discussion

Scheme 1 summarizes the chemical structures of the complexes formed by cholesteryl sulfate sodium salt and the three generations of dendrons, dendrimers, and dendronized polymers. In what follows, we present the structural results of the complexes by each individual dendritic class.

(11) Schlüter, A. D.; Rabe, J. P. *Angew. Chem., Int. Ed.* **2000**, *39*, 864–883.
(12) Frauenrath, H. *Prog. Polym. Sci.* **2005**, *30*, 325–384.
(13) Rudick, J. G.; Percec, V. *Acc. Chem. Res.* **2008**, *41*, 1641–1652.
(14) Rosen, B. M.; Wilson, C. J.; Wilson, D. A.; Peterca, M.; Imam, M. R.; Percec, V. *Chem. Rev.* **2009**, *109*, 6275–6540.
(15) Kato, T.; Mizoshita, N.; Kishimoto, K. *Angew. Chem., Int. Ed.* **2006**, *45*, 38–68.
(16) Canilho, N.; Kasëmi, E.; Mezzenga, R.; Schlüter, A. D. *J. Am. Chem. Soc.* **2006**, *128*, 13998–13999.
(17) Canilho, N.; Kasëmi, E.; Schlüter, A. D.; Mezzenga, R. *Macromolecules* **2007**, *40*, 2822–2830.
(18) Canilho, N.; Kasëmi, E.; Schlüter, A. D.; Ruokolainen, J.; Mezzenga, R. *Macromolecules* **2007**, *40*, 7609–7616.
(19) Mezzenga, R.; Ruokolainen, J.; Canilho, N.; Kasëmi, E.; Schlüter, D. A.; Lee, W. B.; Fredrickson, G. H. *Soft Matter* **2009**, *5*, 92–97.
(20) Lee, W. B.; Elliott, R.; Mezzenga, R.; Fredrickson, G. H. *Macromolecules* **2009**, *42*, 849–859.
(21) Canilho, N.; Kasëmi, E.; Schlüter, A. D.; Ruokolainen, J.; Mezzenga, R. *Macromol. Symp.* **2008**, *270*, 58–64.
(22) Hembury, G. A.; Borovkov, V. V.; Inoue, Y. *Chem. Rev.* **2008**, *108*, 1–73.
(23) Yashima, E.; Maeda, K.; Okamoto, Y. *Nature* **1999**, *399*, 449–451.
(24) Rasberry, R. D.; Wu, X. Y.; Bullock, B. N.; Smith, M. D.; Shimizu, K. D. *Org. Lett.* **2009**, *11*, 2599–2602.
(25) Hase, Y.; Ishikawa, M.; Muraki, R.; Maeda, K.; Yashima, E. *Macromolecules* **2006**, *39*, 6003–6008.
(26) Hasegawa, T.; Maeda, K.; Ishiguro, H.; Yashima, E. *Polym. J.* **2006**, *38*, 912–919.
(27) Ishikawa, M.; Maeda, K.; Mitsutsuji, Y.; Yashima, E. *J. Am. Chem. Soc.* **2004**, *126*, 732–733.
(28) Maeda, K.; Morino, K.; Okamoto, Y.; Sato, T.; Yashima, E. *J. Am. Chem. Soc.* **2004**, *126*, 4329–4342.
(29) Morino, K.; Asari, T.; Maeda, K.; Yashima, E. *J. Polym. Sci., Part A: Polym. Chem.* **2004**, *42*, 4711–4722.
(30) Morino, K.; Watase, N.; Maeda, K.; Yashima, E. *Chem.—Eur. J.* **2004**, *10*, 4703–4707.
(31) Onouchi, H.; Kashiwagi, D.; Hayashi, K.; Maeda, K.; Yashima, E. *Macromolecules* **2004**, *37*, 5495–5503.
(32) Onouchi, H.; Miyagawa, T.; Furuko, A.; Maeda, K.; Yashima, E. *J. Am. Chem. Soc.* **2005**, *127*, 2960–2965.
(33) Yu, Z. N.; Wan, X. H.; Zhang, H. L.; Chen, X. F.; Zhou, Q. F. *Chem. Commun.* **2003**, 974–975.
(34) Ishi-i, T.; Crego-Calama, M.; Timmerman, P.; Reinhoudt, D. N.; Shinkai, S. *J. Am. Chem. Soc.* **2002**, *124*, 14631–14641.
(35) Buono, A. M.; Immediata, I.; Rizzo, P.; Guerra, G. *J. Am. Chem. Soc.* **2007**, *129*, 10992–10993.
(36) Ishikawa, M.; Taura, D.; Maeda, K.; Yashima, E. *Chem. Lett.* **2004**, *33*, 550–551.
(37) Chin, J.; Chong, Y. S.; Bobb, R.; Studnicki, L.; Hong, J. I. *Chem. Commun.* **2007**, 120–122.
(38) Percec, V.; Dulcey, A. E.; Balagurusamy, V. S. K.; Miura, Y.; Smidrkal, J.; Peterca, M.; Nummelin, S.; Edlund, U.; Hudson, S. D.; Heiney, P. A.; Duan, H.; Magonov, S. N.; Vinogradov, S. A. *Nature* **2004**, *430*, 764–768.
(39) Percec, V.; Imam, M. R.; Peterca, M.; Wilson, D. A.; Graf, R.; Spiess, H. W.; Balagurusamy, V. S. K.; Heiney, P. A. *J. Am. Chem. Soc.* **2009**, *131*, 7662–7677.
(40) Percec, V.; Imam, M. R.; Peterca, M.; Wilson, D. A.; Heiney, P. A. *J. Am. Chem. Soc.* **2008**, *131*, 1294–1304.
(41) Percec, V.; Dulcey, A. E.; Peterca, M.; Ilies, M.; Nummelin, S.; Sienkowska, M. J.; Heiney, P. A. *Proc. Natl. Acad. Sci. U.S.A.* **2006**, *103*, 2518–2523.
(42) Percec, V.; Peterca, M.; Rudick, J. G.; Aqad, E.; Imam, M. R.; Heiney, P. A. *Chem.—Eur. J.* **2007**, *13*, 9572–9581.
(43) Percec, V.; Rudick, J. G.; Peterca, M.; Aqad, E.; Imam, M. R.; Heiney, P. A. *J. Polym. Sci., Part A: Polym. Chem.* **2007**, *45*, 4974–4987.
(44) Tsiourvas, D.; Felekis, T.; Sideratou, Z.; Paleos, C. M. *Liq. Cryst.* **2004**, *31*, 739–744.

Scheme 1. Schematic Drawing of Dendrons (DD*n*, *n* = number of generation), Dendrimers (DM*n*), Dendronized Polymers (DP*n*), and Cholesteryl Sulfate Unit Used in the Present Study[a]

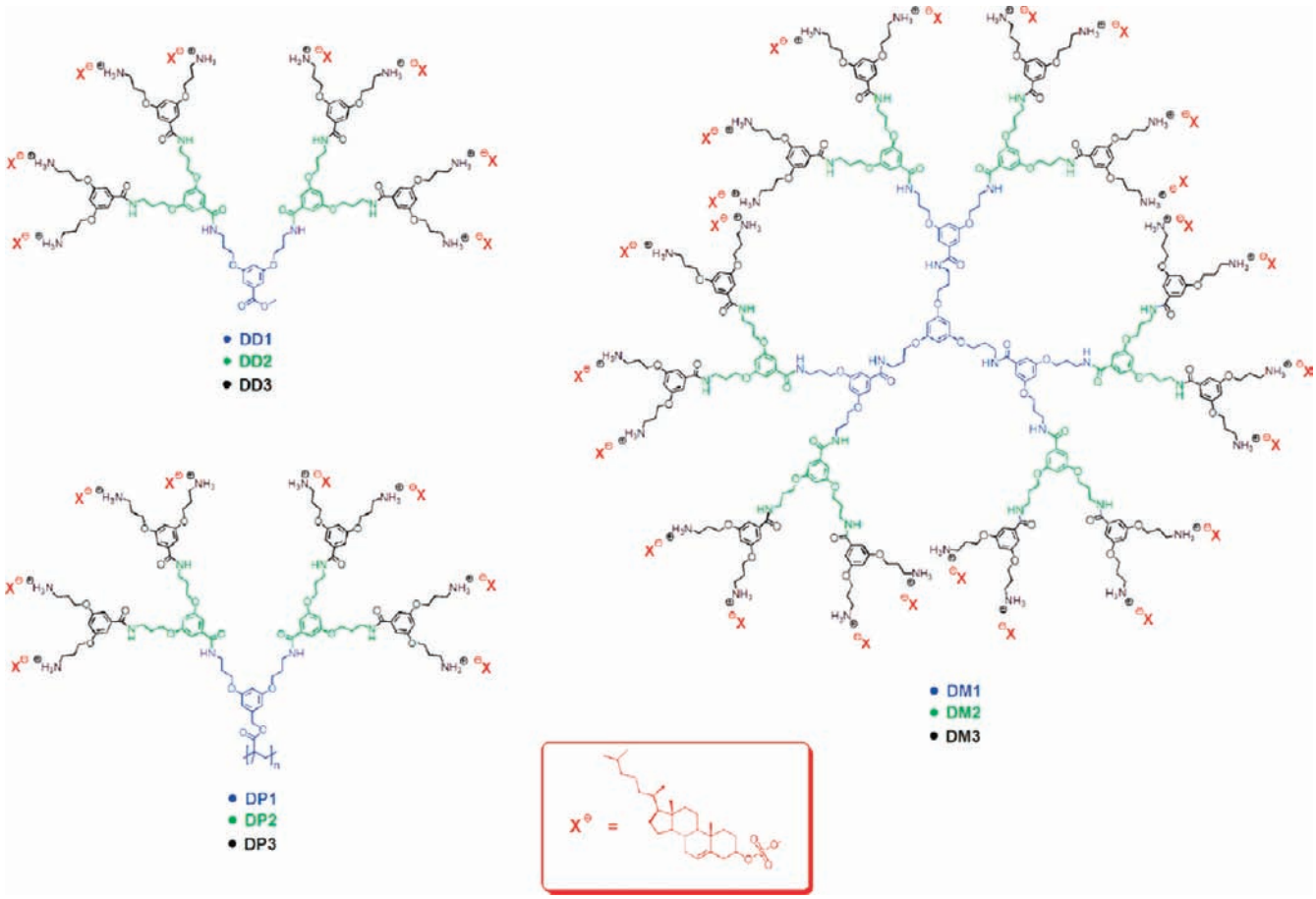

[a] Only third-generation molecules are entirely drawn; the corresponding first and second generations (excluding ammonium charges) are highlighted in blue and green, respectively. X identifies the cholesteryl sulfate sodium salt unit already dissociated from the Na^+ counterion and is highlighted in red.

Dendrons. Dendrons are the smallest molecules used in this study. They are also the basic building blocks of the other dendritic molecules studied in this paper. Figure 1a shows a TEM image of the first-generation dendron complex (DD1−Chol). The morphology is clearly lamellar, which is also confirmed by the evenly spaced SAXS peaks shown in Figure 1b. The period of the lamellar spacing is 4.8 nm according to SAXS, which agrees well with 4.9 nm given by TEM analysis. The high-magnification inset in Figure 1a reveals the presence of undulations in the lamellar phase.

The second-generation dendron complex DD2−Chol has columnar morphology, in which the cylinders are organized in a hexagonal lattice, as clearly shown in the corresponding TEM image in Figure 2a. The hexagonal arrangement of the columns is also confirmed by SAXS. In the diffractogram shown in Figure 2b, the scattering peaks are spaced as $1:\sqrt{3}:2:\sqrt{7}:3:\sqrt{12}:\sqrt{13}$, which is a characteristic feature of hexagonal systems. The lattice parameter *a* is extracted to be 9.0 nm, which is consistent with the 8.9 nm measured in TEM.

The atypical structure factor of the diffractogram in Figure 2b, with the second Bragg reflection being the most intense, also suggests nontrivial hexagonal columnar packing. A similar scattering profile has been recently reported by Merlet-Lacroix et al.[45] in core−shell hexagonally packed cylinders based on another class of dendritic supramolecular ionic complexes. Consistently, the inset in Figure 2a reveals that the cylinders contain a dotlike clear domain in the center, resembling a core−shell system. Since RuO_4 stains the aromatic rings of the dendrons, it is obvious to identify the dark circular domains in the electron micrographs with the dendrons. Volume fraction considerations would strongly support the cholesteric units forming the continuous honeycomblike light domains, since the size of the "light spots" in the center appears to be too small to allow their identification with the cholesteric units. Thus, we propose that the light spots in the center of the columns are low electron density domains composed of the focal points of the dendrons. Hexagonally packed cylinders with low electron contrast cores have been previously reported in chiral block copolymers as a result of macromolecule-induced chirality, which would systematically twist the molecular arrangement forming the cylinders.[46−48] A similar interpretation, together with the CD data to be discussed later in this report, would also support the same twisted self-assembly scheme in the present complex. Macromolecular chirality along the cylinder's axis would actually enhance this contrast. A possible structure

(45) Merlet-Lacroix, N.; Rao, J.; Schlüter, D.; Bolisetty, S.; Ruokolainen, J.; Mezzenga, R. *Macromolecules* **2010**, *43*, 4752–4760.
(46) Ho, R.-M.; Chen, C.-K.; Chiang, Y.-W. *Macromol. Rapid Commun.* **2009**, *30*, 1439–1456.
(47) Ho, R.-M.; Chiang, Y.-W.; Tsai, C.-C.; Lin, C.-C.; Ko, B.-T.; Huang, B.-H. *J. Am. Chem. Soc.* **2004**, *126*, 2704–2705.
(48) Ho, R.-M.; Tseng, W.-H.; Fan, H.-W.; Chiang, Y.-W.; Lin, C.-C.; Ko, B.-T.; Huang, B.-H. *Polymer* **2005**, *46*, 9362–9377.

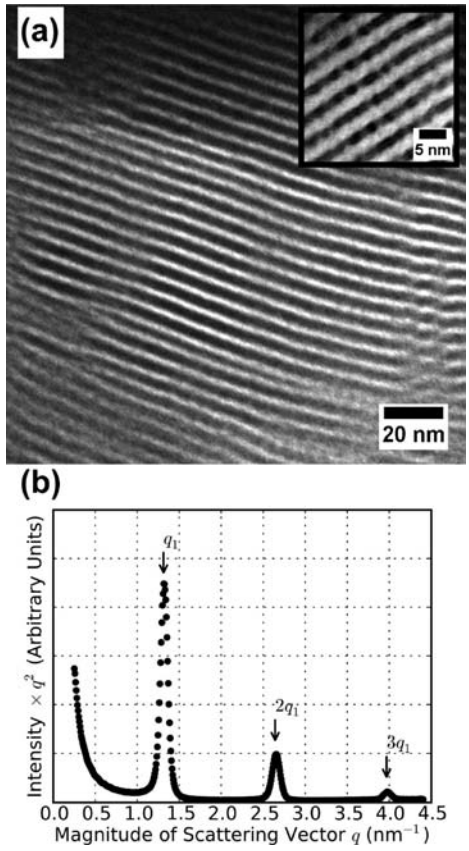

Figure 1. (a) Transmission electron microscopic image of the first-generation dendron complex (DD1−Chol), showing a clear lamellar structure. (Inset) Undulations of the lamellae at the length scale of individual layers (~3 nm). (b) Lorentz-corrected SAXS diffractogram of DD1−Chol, showing evenly spaced scattering peaks, which is a typical feature of lamellar morphology.

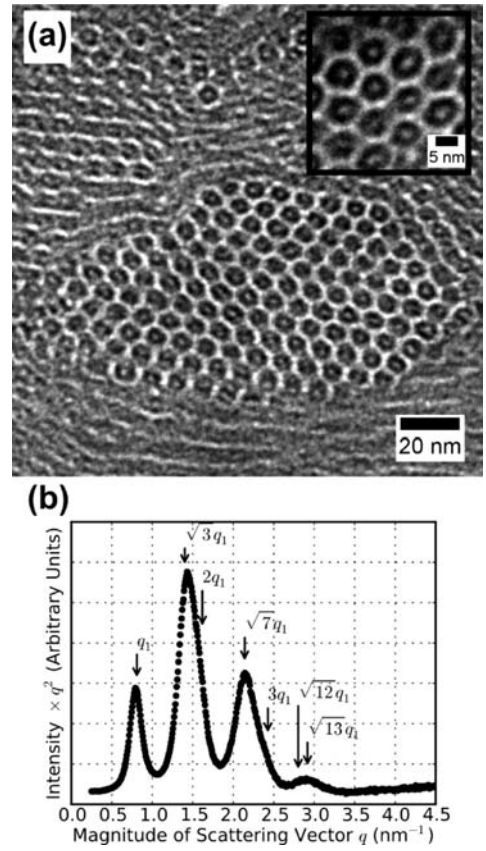

Figure 2. (a) Transmission electron microscopic image of the second-generation dendron complex (DD2−Chol), which has hexagonal columnar structure. (Inset) Higher magnification image, which is taken orthogonal to the column axis. (b) Hexagonal ordering is also confirmed by the Lorentz-corrected SAXS diffractogram, in which the scattering peaks are spaced as $1:\sqrt{3}:2:\sqrt{7}:3:\sqrt{12}:\sqrt{13}$.

consistent with this self-assembly model is schematically shown in Figure 3. To find out whether the low electron density cylinder cores actually correspond to empty space, a separate Brunauer−Emmett−Teller (BET) analysis was carried out. This analysis, however, demonstrated that these samples are compact and they do not exhibit any porosity. The measured adsorption and desorption isotherms (see Supporting Information) were of type III, which is characteristic for nonporous or macroporous materials. The pore volume calculated by the BET method was below 0.01 cm^3/g.

The third-generation dendron is the largest and bulkiest of the dendrons discussed here. The structure of its cholesteryl complex DD3−Chol, while poor in long-range order, is similar to the second-generation complex DD2−Chol as seen in the TEM image shown in Figure 4. However, the positions of SAXS peaks of the complex do not coincide with a regular columnar hexagonal pattern, which suggests an alternative packing structure of the cylinders or simply a more distorted lattice.

A possible structure that could explain the features seen in both TEM images and SAXS diffractograms is the oblique columnar structure. Its lattice vectors and parameters are shown in Figure 5. The unit cell of the oblique columnar structure is defined by two lattice parameters a and b and an angle γ. In order to find the lattice parameters for the third-generation dendron complex, a simple method for fitting the scattering peak positions based on work by Zhou et al.[49] was used. Although the method does not allow fitting of the intensity of the experimental curve with the effective structure factors, it enables one to compare the peak positions. The model assumes a simple total scattering intensity

$$I(q) = \langle \sum_{h,k} I_{hk}(|\mathbf{q} - h\mathbf{a}^* - k\mathbf{b}^*|) \rangle_{\text{spherical}} = \sum_{h,k} \frac{1}{4\pi q_{hk}^2} I_{hk}(q - q_{hk}) \quad (1)$$

where $\langle ... \rangle_{\text{spherical}}$ denotes a spherical average, q is the magnitude of the scattering vector $\mathbf{q}$, I_{hk} is the scattering intensity from the two-dimensional scattering plane defined by the indices h and k, $\mathbf{a}^*$ and $\mathbf{b}^*$ are the reciprocal lattice vectors, and q_{hk} is the magnitude of the scattering vector from the (hk) plane.

For the oblique columnar structure assumed here

$$q_{hk} = \frac{2\pi}{\sin\gamma}\sqrt{\frac{h^2}{a^2} - \frac{2hk\cos\gamma}{ab} + \frac{k^2}{b^2}} \quad (2)$$

We chose the individual scattering intensities I_{hk} to be of Gaussian peak shape with predefined width and normalized height. Therefore, details like crystallite sizes, lattice distortions,

(49) Zhou, S.; Hu, H.; Burger, C.; Chu, B. *Macromolecules* **2001**, *34*, 1772–1778.

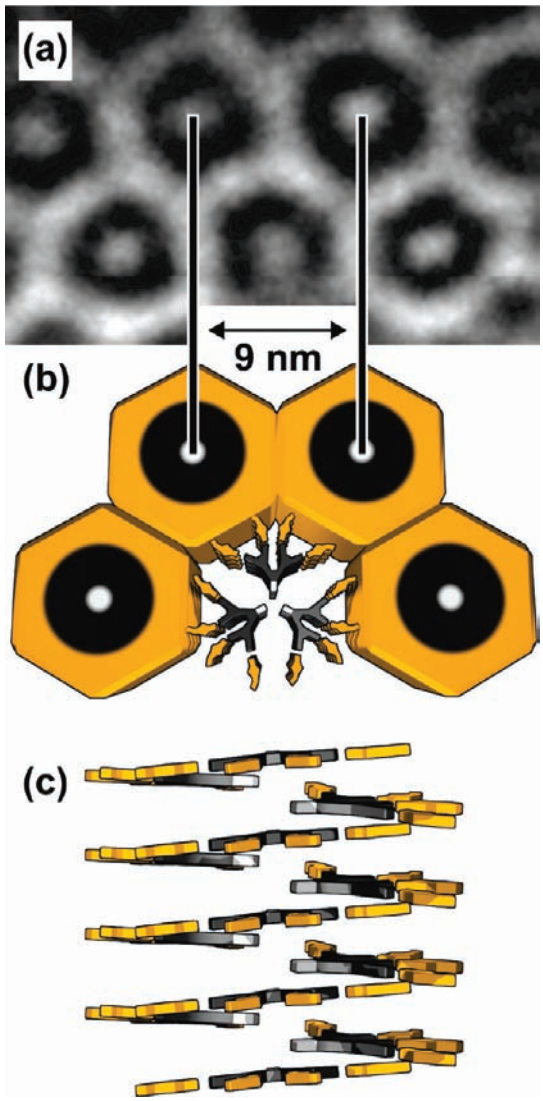

Figure 3. (a) Transmission electron microscopic image of hexagonal columnar morphology found in the second-generation dendron complex (DD2−Chol) and (b) its schematic representation. The low electron contrast focal points of the dendritic molecules are in the center of the columns while the cholesteric pendant groups occupy the coronas. (c) A twisted arrangement of the supramolecules along the column axis is suggested by CD measurements.

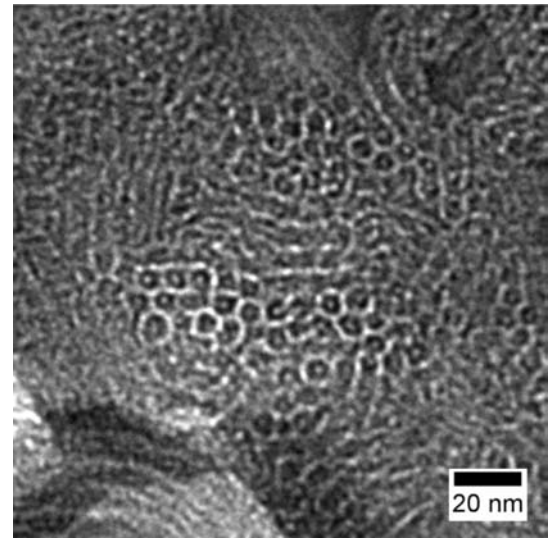

Figure 4. Transmission electron microscopic image showing short-range order of the columnar structure of the third-generation dendron complex (DD3−Chol).

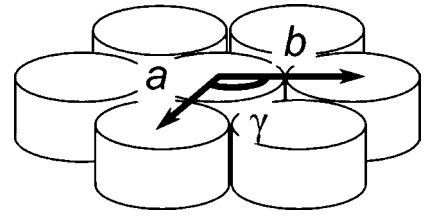

Figure 5. Unit cell of an oblique columnar structure, defined by two lattice parameters a and b and an angle γ.

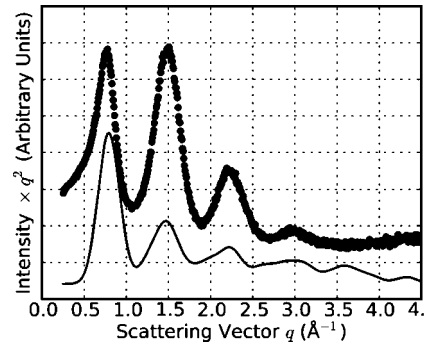

Figure 6. Lorentz-corrected small-angle X-ray diffractogram (black dots) of the third-generation dendron complex (DD3−Chol). The solid line is a computed intensity for an oblique columnar structure for which the positions of the four highest intensity scattering peaks have been fitted to the measured data.

or device factors that make the widths of the peaks dependent on the scattering vector are not included in the model. The algorithm works as follows: starting from initial lattice parameters a and b and angle γ, the Nelder−Mead simplex method is used to minimize the sum of squared differences between Lorentz-corrected peak positions in the experimental data and the corresponding peak positions in calculated I. During computations, the indices h and k were limited in the range [−5 ... +5], because considering higher indices did not affect the results. As can be seen in Figure 5, hexagonal columnar structure is a special case of oblique columnar where $a = b$ and $\gamma = 120°$. Since the TEM images of DD3−Chol are similar to those of the second-generation complex, we expect to find lattice parameters close to the values of the hexagonal morphology, namely, $a \approx b$ and $\gamma \approx 120°$. This is indeed the case: the fitting algorithm gives lattice parameters $a = 9.9$ nm, $b = 8.8$ nm, and $\gamma = 124°$. The Bragg reflections are correctly reproduced as can be seen in Figure 6. In the measured data, the highest deviation in peak intensities arises, as expected, in the second Bragg reflection, as a consequence of the nonconventional form factor of the core−shell-type cylinders.[45] Also, the parameters are consistent with TEM analysis in which a and b are approximately 8−9 nm. Therefore, we infer that the structure is of the oblique columnar type.

Dendrimers. The dendrimer molecules are formed by attaching three dendrons together from their focal points, and accordingly, they have three times the functional peripheral groups of the corresponding dendron generation. Thus, it is not

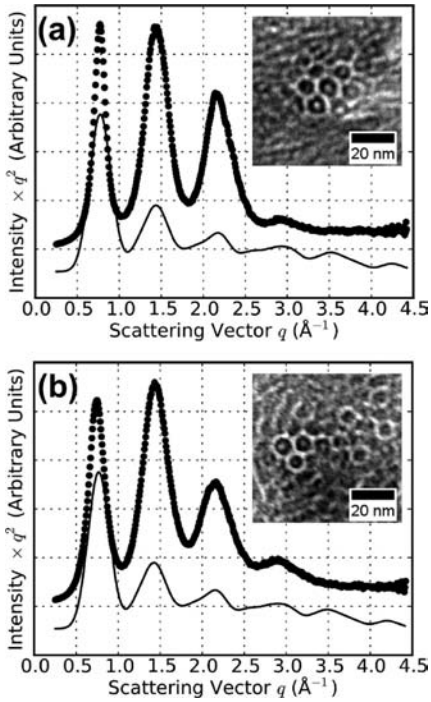

Figure 7. Small-angle X-ray scattering diffractograms (black dots) for (a) the first-generation dendrimer complex (DM1−Chol) and (b) the second-generation dendrimer complex (DM2−Chol), showing scattering peaks at positions that do not correspond to the characteristic positions of conventional structures. The positions of the four highest intensity peaks of the computed intensity curve of oblique columnar structures (solid lines) have been fitted to the positions of the peaks of the measured data. The TEM images in the insets show the "core-shell" structure of the columnar structures.

a surprise to find some analogies between the morphologies of the dendrimer and the dendron complexes. A first difference, however, arises when the first-generation homologous complexes are compared: while in the case of DD1−Chol a lamellar phase is found (Figure 1), in the case of DM1−Chol (see Figure 7a) a structure similar to the columnar morphologies of the higher-generation dendron complexes is observed. The second-generation homologous dendrons and dendrimers cases (Figures 2 and 7b, respectively) are more directly comparable. In transmission electron microscopy, DM2−Chol appears again as a core−shell-like columnar structure with light coronas, and a central spot within dark cylinders can be observed (see the inset in Figure 7b). However, the structure is not as well ordered as DD2−Chol and the micrographs are reminiscent of the DD3−Chol complex where the oblique columnar morphology was observed. Indeed, SAXS peak positions suggest a similar morphology for both DM1−Chol and DM2−Chol. Therefore, the same fitting procedure as described for DD3−Chol was used to resolve the lattice parameters from the SAXS data for the DM1−Chol and DM2−Chol complexes. The diffractograms and fitted intensities are shown in Figure 7. The fitting procedure results in lattice parameters $a = 10.2$ nm, $b = 9.0$ nm, and $\gamma = 124°$ for both DM1−Chol and DM2−Chol. Thus, the generation does not seem to considerably affect the lattice parameters. Tentatively, these results can be explained with a more pronounced tilt of DM2−Chol "disklike" complexes with respect to the main columnar axis as compared to DM1−Chol complexes, yielding virtually identical lattice parameters.

The third-generation dendrimer complex DM3−Chol, the largest of the dendrimers, shows a microphase-separated state

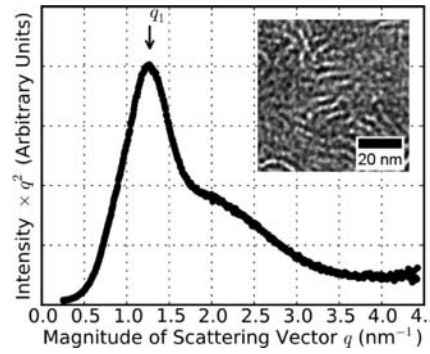

Figure 8. Small-angle X-ray scattering diffractogram of the third-generation dendrimer complex (DM3−Chol), showing only one distinguishable scattering peak, with a higher q shoulder. (Inset) Transmission electron microscopic image of the wormlike structure of the complex.

distinguishingly different from the first- and second-generation dendrimers. The structure has very short-range order, as revealed by both TEM and the SAXS diffractogram (Figure 8). A broad SAXS peak centered at 1.27 nm^{-1} corresponds to a period of 4.9 nm, which is consistent with the "wormlike" structure with the 4.7 nm period observed in TEM.

Taken together, the SAXS and TEM data for the dendrimer complexes reveal a decreased level of order when compared to the homologous dendron complex series. The reasons for such a decreased structural order in the solid state have to be searched on the topological restrictions imposed on three dendrons when connected into a single dendrimer: it is evident that this results in a restriction of the original 3^3 degrees of freedom of the three dendrons' focal points to 3^1 degrees of freedom of the single core of the dendrimer. These topological restrictions might very well explain the reduced order achieved by the dendrimer complexes in the solid state when compared with the dendrons. This argument will be further reinforced by the study of the dendronized polymer complexes presented in what follows.

Dendronized Polymers. The dendronized polymers studied here are formed by polymerizing the dendron molecules from their focal point. As they are the largest and bulkiest class of molecules in this study, it comes as no surprise that the dendronized polymers exhibit the least ordered structures. In the TEM images the three dendronized polymer generations DP1−Chol, DP2−Chol, and DP3−Chol, a microphase-separated wormlike structure can be identified as shown in the insets of Figure 9. All three generations have two scattering maxima in their SAXS diffractograms. Again, the separation of the scattering peak positions does not fit with conventional hexagonal or lamellar patterns. Since there are only two distinguishable scattering peaks, a fit based on the method used previously with the oblique columnar structures would not be justified because of its three independent parameters. Therefore, we interpret the structures to be of the rectangular columnar type where $\gamma = 90°$ and $a \neq b$. For rectangular columnar structure

$$q_{hk} = 2\pi\sqrt{\frac{h^2}{a^2} + \frac{k^2}{b^2}} \tag{3}$$

This structure has been also found in a previous study for the same dendronized polymers complexed with lipids[17] and is

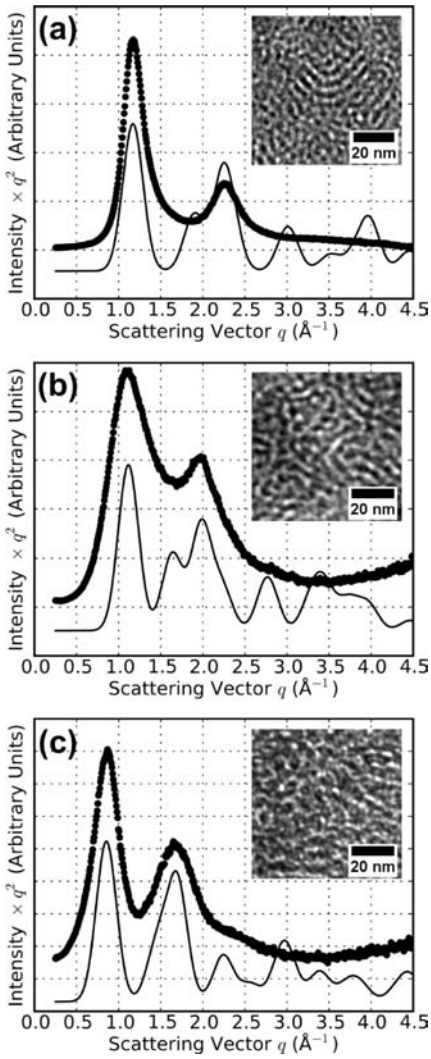

Figure 9. Small-angle X-ray scattering diffractograms of (a) the first- (DP1−Chol), (b) second- (DP2−Chol), and c) third-generation (DP3−Chol) dendronized polymer complexes drawn with black dots. The solid lines are computed intensity curves, peak positions of which have been fitted to the experimental data.

not uncommon in other helical supramolecular systems.[50] Fitting to the SAXS peaks gives computed intensities shown along with the measured data in Figure 9. The parameters resulting from the fitting for first-generation dendronized polymer complex (DP1−Chol) are $a = 5.4$ nm and $b = 3.3$ nm and for the second-generation complex (DP2−Chol), $a = 5.6$ nm and $b = 3.8$ nm. These values are consistent with TEM analysis, which shows structures of approximately 5 nm in size for DP1−Chol and DP2−Chol, and are very similar to the lattice parameters reported for the rectangular phases found in supramolecular dendronized polymer−lipid complexes.[17] The difference between the lattice vector lengths of these two dendritic polymers is due to the higher generation and thus larger dendritic side chains of DP2−Chol. The trend continues with the third-generation dendronized polymer: fitting gives lattice parameters $a = 7.4$ nm and $b = 4.3$ nm, while TEM gives a period of approximately 7 nm.

The poor order observed in the dendronized polymer systems can be rationalized once more in terms of the topological restrictions imposed by the spatial arrangement of dendron−cholesteryl moieties in the solid state, once these are attached to a common backbone. In this case, any three consecutive dendrons along the backbone not only are attached covalently through their focal point to a common polymer backbone but also have the focal points aligned along the same linear contour length. Because the consecutive grafting distances are fixed, the only degree of freedom remaining is the position of grafting along the polymer backbone. In other words, for any n dendrons, the degrees of freedom of the corresponding focal points are $3^n \rightarrow 3^{n/3} \rightarrow n/3$ when going from dendrons → dendrimers → dendronized polymers.

It is to be expected that further topological bond restrictions occurring in both dendrimers and dendronized polymers will additionally reduce the possible packing configurations with respect to the free dendron systems, further depressing the ordering of the corresponding solid-state complexes.

The different dendritic complexes and their structures as revealed by SAXS and TEM analysis are summarized in Table 1.

Table 1. Structures of Dendron, Dendrimer, and Dendronized Polymer Cholesteryl Sulfate Sodium Salt Complexes

type of complex	structure	lattice parameters[a]
	Dendrons	
generation 1	lamellar	4.4 nm
generation 2	hexagonal columnar	$a = b = 9.0$ nm, $\gamma = 120°$
generation 3	oblique columnar	$a = 9.9$ nm, $b = 8.8$ nm, $\gamma = 124°$
	Dendrimers	
generation 1	oblique columnar	$a = 10.2$ nm, $b = 9.0$ nm, $\gamma = 124°$
generation 2	oblique columnar	$a = 10.2$ nm, $b = 9.0$ nm, $\gamma = 124°$
generation 3	microphase-separated	4.7 nm
	Dendronized Polymers	
generation 1	rectangular columnar	$a = 5.4$ nm, $b = 3.3$ nm
generation 2	rectangular columnar	$a = 5.6$ nm, $b = 3.8$ nm
generation 3	rectangular columnar	$a = 7.4$ nm, $b = 4.3$ nm

[a] Lattice parameters for the oblique columnar and rectangular columnar structures are based on the fitting procedure described in the paper.

Circular Dichroism. The ultraviolet/visible light spectrum and circular dichroic signal were acquired from drop-cast films for each individual complex and compared with the corresponding noncomplexed dendritic macromolecule and the cholesteryl sulfate sodium salt. The noncomplexed dendrons, dendrimers, and dendronized polymers absorbed light in the ultraviolet wavelengths with a maximum absorption at approximately 210 nm but did not show significant optical activity in the CD region. The film of chiral cholesteryl sulfate sodium salt had an absorption maximum in the UV region and showed a single minimum value in the CD at approximately 200 nm. All dendritic complexes showed enhanced optical activity with complex CD spectra. Figure 10b compares the UV−vis spectra of the noncomplexed first-generation dendron, the cholesteryl sulfate sodium salt, and their complex (DD1−Chol). Note that the detector was saturated at wavelengths below approximately 210 nm. The corresponding CD signals are shown in Figure 10a. As can be observed, the CD signal appears to be uncorrelated with that of the chiral cholesteryl sulfate sodium salt, with the presence of additional and distinct CD peaks that are not characteristic of the cholesteryl unit alone. This clearly indicates the presence of supramolecule-induced chirality, or induced circular dichroism (ICD). Figure 10 panels d and f show

(50) Huang, Y.; Yan, Y.; Smarsly, B. M.; Wei, Z.; Faul, C. F. J. *J. Mater. Chem.* **2009**, *19*, 2356–2362.

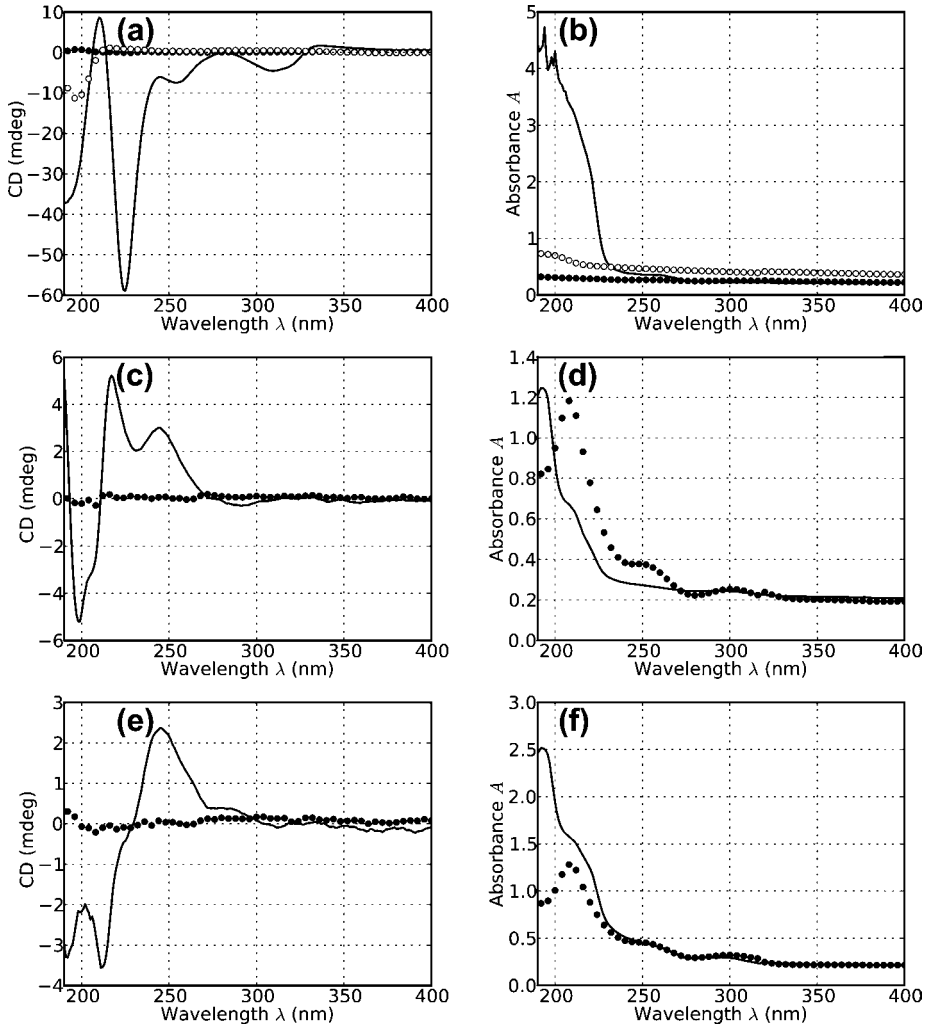

Figure 10. Circular dichroism (CD) and ultraviolet/visible light (UV−vis) absorbance spectra of dendrons (●), cholesteryl sulfate sodium salt (○), and their complexes (—). (a) The induced circular dichroism (ICD) effect is evident when the CD signals of the first-generation dendron and its complex (DD1−Chol) are compared. The signal of the complex is not correlated to either of its constituents. (b) UV−vis spectra of the same complex. Note that the instrument saturated while measuring the absorbance of DD1−Chol below approximately 210 nm. ICD is less pronounced, but still very clear, in the higher-generation dendron complexes as can be seen from the CD and UV−vis spectra for (c, d) second-generation and (e, f) third-generation dendrons and their complexes (DD2−Chol and DD3−Chol), respectively.

the UV−vis absorbance for the second- and third-generation dendron complexes (DD2−Chol and DD3−Chol). Figure 10 panels c and e give the corresponding CD signals, showing again the presence of ICD in the solid state. The CD spectra for all the other complexes investigated are given in the Supporting Information. While the effect is not as pronounced as with dendron complexes, they also exhibited ICD. It turns out to be challenging to correlate the exact CD signal with the solid-state structures observed for the various complexes, but clearly induced circular dichroism occurs in each individual complex with a systematic change in their CD signal. In general, it was observed that the first-generation complexes had more pronounced CD signals, and the higher molecular weight dendritic classes (dendrimers and dendronized polymers) had a lower ICD effect than dendrons. This suggests that molecular mobility in the dendritic complexes and the final level of order achieved in the solid state can play a major role on the establishment of macromolecular chirality. Irrespective of the architecture of the complexes, all columnar phases may be assumed to adopt a helical arrangement similar to that disclosed in Figure 3, which is responsible for the observed macromolecular chirality. The occurrence of induced circular dichroism in the lamellar phases (DD1−Chol) can be thought to arise from chirality-induced undulations of the lamellae, consistent with what is shown in the inset of Figure 1a.

Conclusions

Ionic complexation of chiral cholesteric pendant groups with dendritic macromolecules such as dendrons, dendrimers, and dendronized polymers leads to self-organizing microphase-separated structures as a consequence of the segregation of the cholesteric pendant groups and the dendritic core. Depending on the kind of dendritic molecule and the generation, (i) lamellar, (ii) columnar hexagonal, (iii) oblique columnar, (iv) rectangular columnar, and (v) short-range ordered microphase-separated morphologies are observed by small-angle X-ray scattering (SAXS) and transmission electron microscopy (TEM) studies. A general trend is that the level of order achieved in the solid state is directly correlated with the degrees of freedom of the dendritic macromolecular template used. Accordingly, the order in self-assembled structures of the complexes in the solid state is found to decrease when going from dendron → dendrimer

→ dendronized polymer complexes. A particular feature of the columnar systems, which can be revealed by TEM, is that the dendritic molecules are positioned in such a way that the cholesteric units occupy the column shells while the focal points of the dendrons and dendrimers are in the center of the columns. This structural feature differs from the topological organization found in inverted columnar phases obtained by the same dendritic macromolecules complexed with smaller and softer sulfate alkyl tail nonchiral surfactants,[18,19] inferring the role of volume fraction, rigidity, and chirality in the molecular packing of the complexes in the solid state. Finally, the columns are dense and do not exhibit a central cavity as demonstrated by porosity measurements (BET).

Compared to the noncomplexed dendritic molecules, optical activity in the solid state showed a change in ultraviolet/visible light (UV−vis) absorption and a systematic increase in the CD signal, indicating the occurrence of supramolecular chirality induced by the complexation of the achiral dendritic macromolecules with the chiral cholesteric moieties. Enhancement of the optical signals appear to be correlated with the order of the structure in the solid state, because complexes that exhibit the highest structural order in the solid state also show the most enhanced CD signal.

Acknowledgment. The Finnish Academy of Science and the Swiss National Science Foundation are kindly acknowledged for financial support.

Supporting Information Available: Descriptions of experimental methods, materials and synthesis; transmission electron micrographs of the dendronized polymer complexes (DP1−Chol, DP2−Chol, DP3−Chol); circular dichroism and ultraviolet/visible light spectra of the dendrimer complexes (DM1−Chol, DM2−Chol, DM3−Chol) and the dendronized polymer complexes (DP1−Chol, DP2−Chol, DP3−Chol); and nitrogen adsorption and desorption isotherms of the second-generation dendron complex (DD2−Chol). This material is available free of charge via the Internet at http://pubs.acs.org.

JA103754D